X-ray pulsars at very low luminosity state

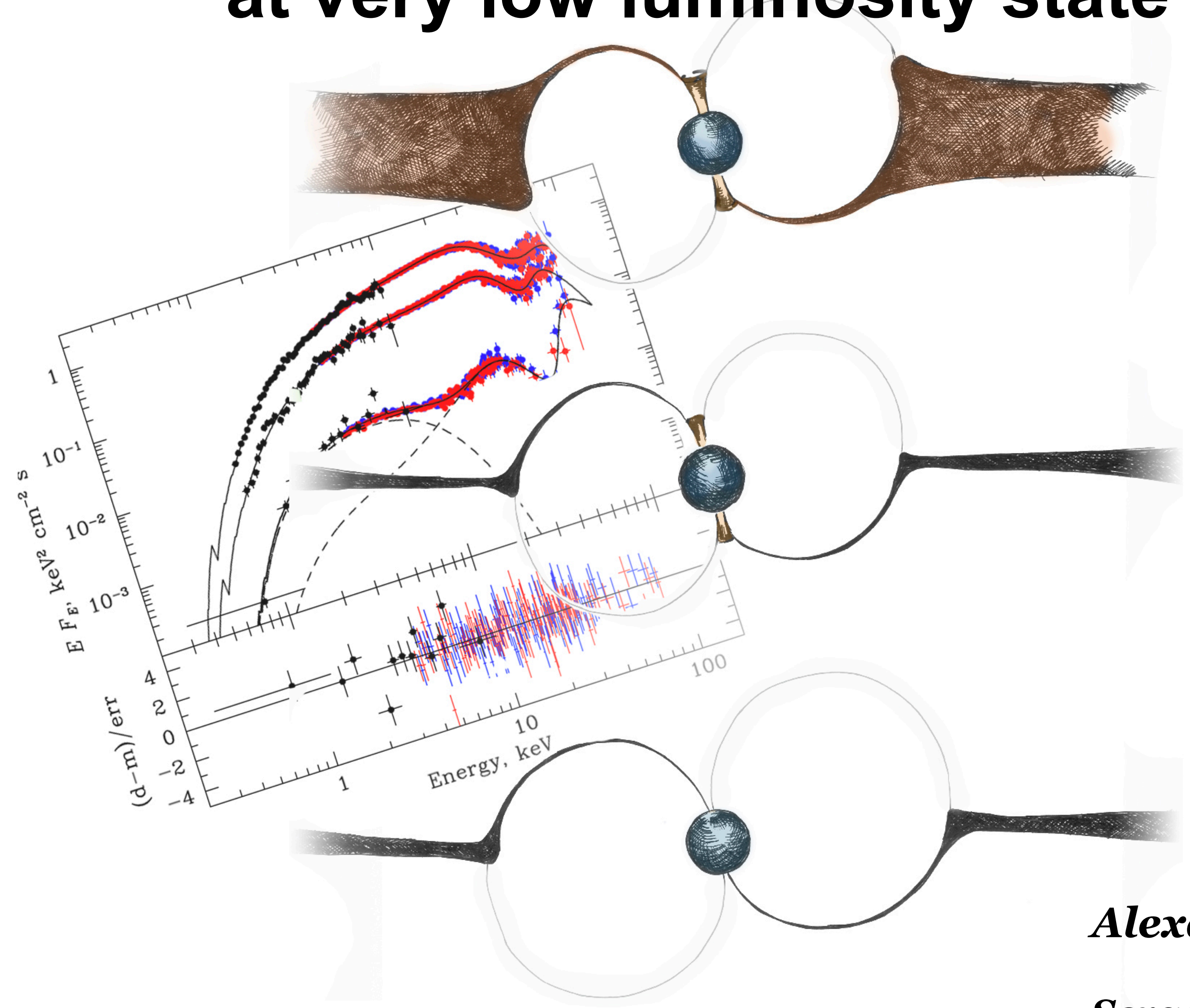

Alexander Mushtukov

Sergey S. Tsygankov
Valery F. Suleimanov
Victor Doroshenko
Alexander Lutovinov
Juri Poutanen

Universiteit Leiden

ИКИ

Главная (Пулковская) астрономическая обсерватория РАН

X-ray pulsar

Rotating Neutron Star in binary systems

Neutron star parameters:

M_{NS}~1.5-2 M_{sun}

R_{NS} ~10-15 km

P_{spin} ~1 – 10^3 s

B_{NS} ~10^{12} G

X-ray pulsar

Typical spectra

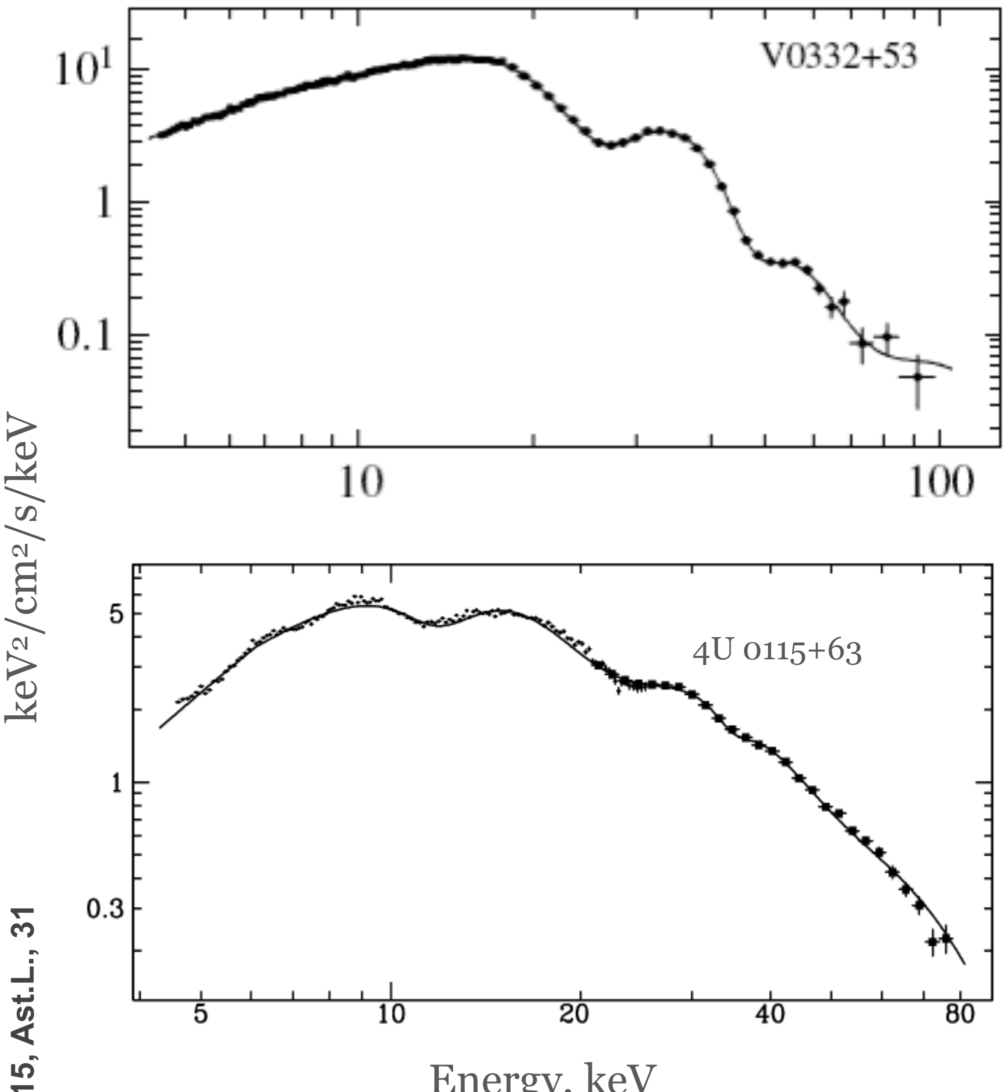

Source name	Cyclotron energy, keV
4U 0115+63 (–)	11.5, 20.1, 33.6, 49.5, 53
V 0332+53 (–)	28, 53, 74
4U 0352+309 (X Per)	29
RX J0440.9+4431	32
RX J0520.5-6932	31.5
A 0535+262	50, 110
MXB 0656–072	36
Vela X-1 (+)	27,54
GRO J1008-57	88?, 75.5
1A 1118–61	55
Cen X-3	28
GX 301–2	37, 48
GX 304–1 (+)	50.8
4U 1538–52	20, 47
Swift J1626.6–5156	10
4U 1626–67	37
Her X-1 (+)	42
OAO 1657–415	36
GRO J1744–28	4.7
IGR J18179–1621	21
GS 1843+00	20
4U 1907+09	19, 40
4U 1909+07	44?
XTE J1946+274	36
KS 1947+300	12.5
EXO 2030+375	11?, 36?, 63?
Cep X-4	30

$$E_{\rm cyc} = 11.6\, B_{12}\, {\rm keV}$$

Filippova+, 2015, Ast.L., 31

X-ray pulsar

Typical spectra

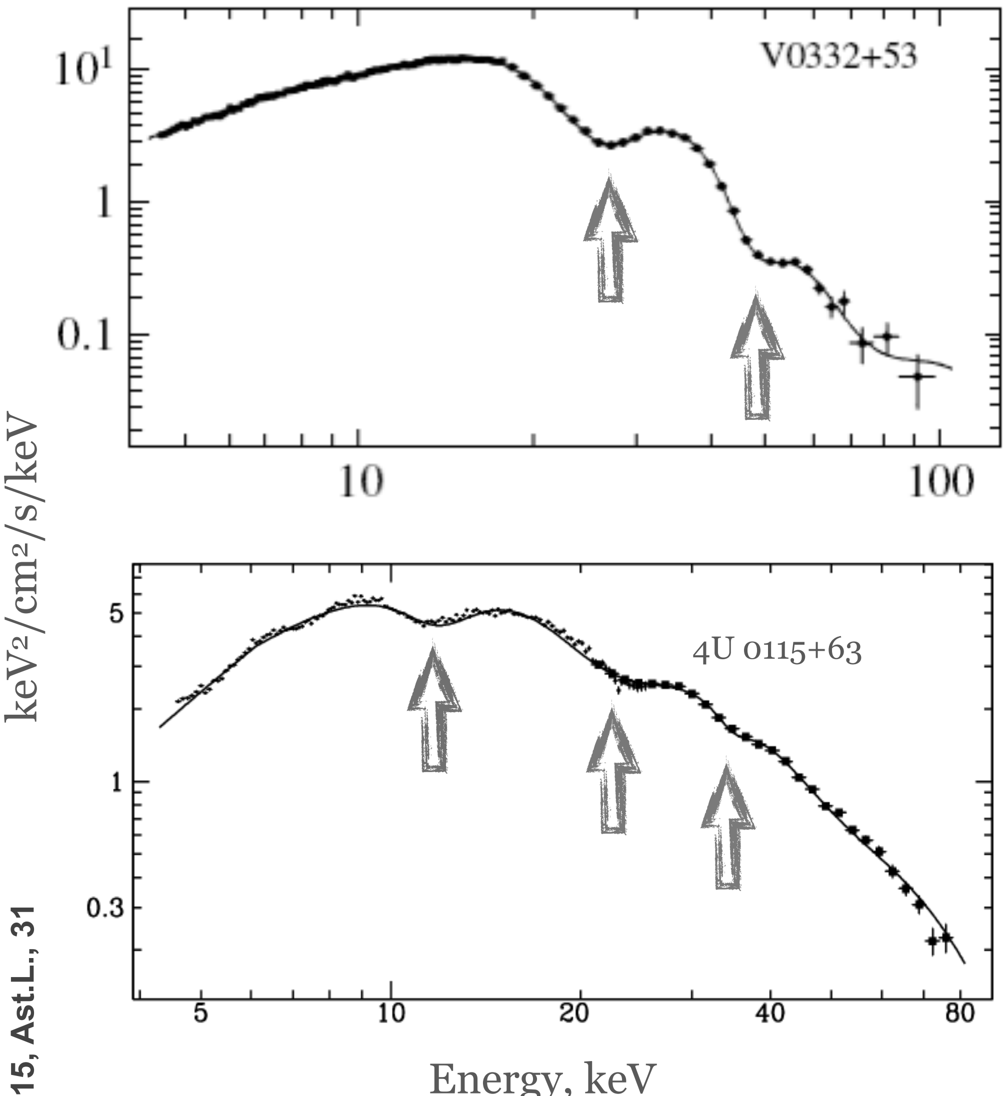

Source name	Cyclotron energy, keV
4U 0115+63 (–)	11.5, 20.1, 33.6, 49.5, 53
V 0332+53 (–)	28, 53, 74
4U 0352+309 (X Per)	29
RX J0440.9+4431	32
RX J0520.5-6932	31.5
A 0535+262	50, 110
MXB 0656–072	36
Vela X-1 (+)	27,54
GRO J1008-57	$88^?$, 75.5
1A 1118–61	55
Cen X-3	28
GX 301–2	37, 48
GX 304–1 (+)	50.8
4U 1538–52	20, 47
Swift J1626.6–5156	10
4U 1626–67	37
Her X-1 (+)	42
OAO 1657–415	36
GRO J1744–28	4.7
IGR J18179–1621	21
GS 1843+00	20
4U 1907+09	19, 40
4U 1909+07	$44^?$
XTE J1946+274	36
KS 1947+300	12.5
EXO 2030+375	$11^?$, $36^?$, $63^?$
Cep X-4	30

$$E_{\rm cyc} = 11.6\, B_{12}\, {\rm keV}$$

Filippova+, 2015, Ast.L., 31

Transients

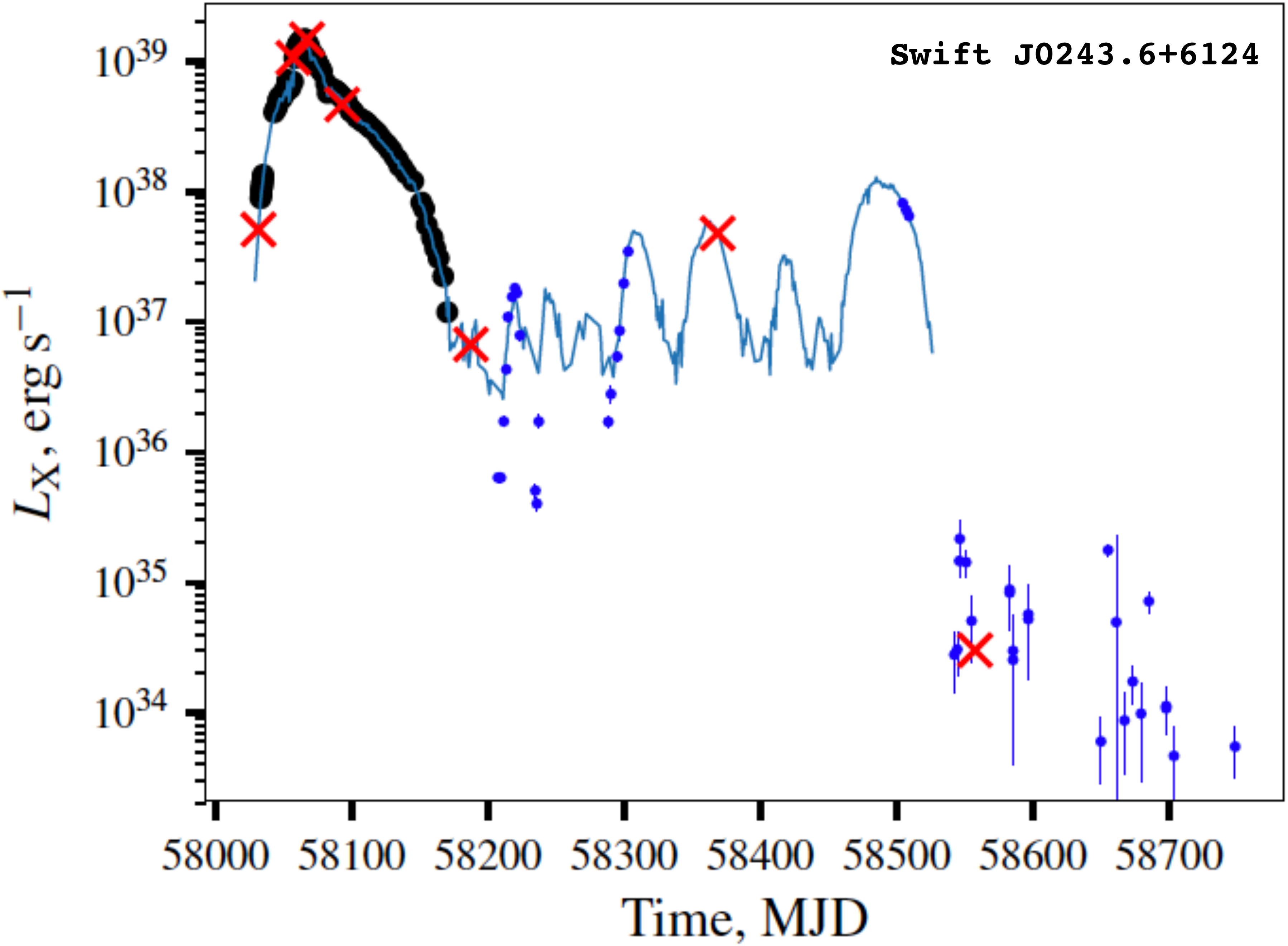

Doroshenko+, 2019, MNRAS, accepted

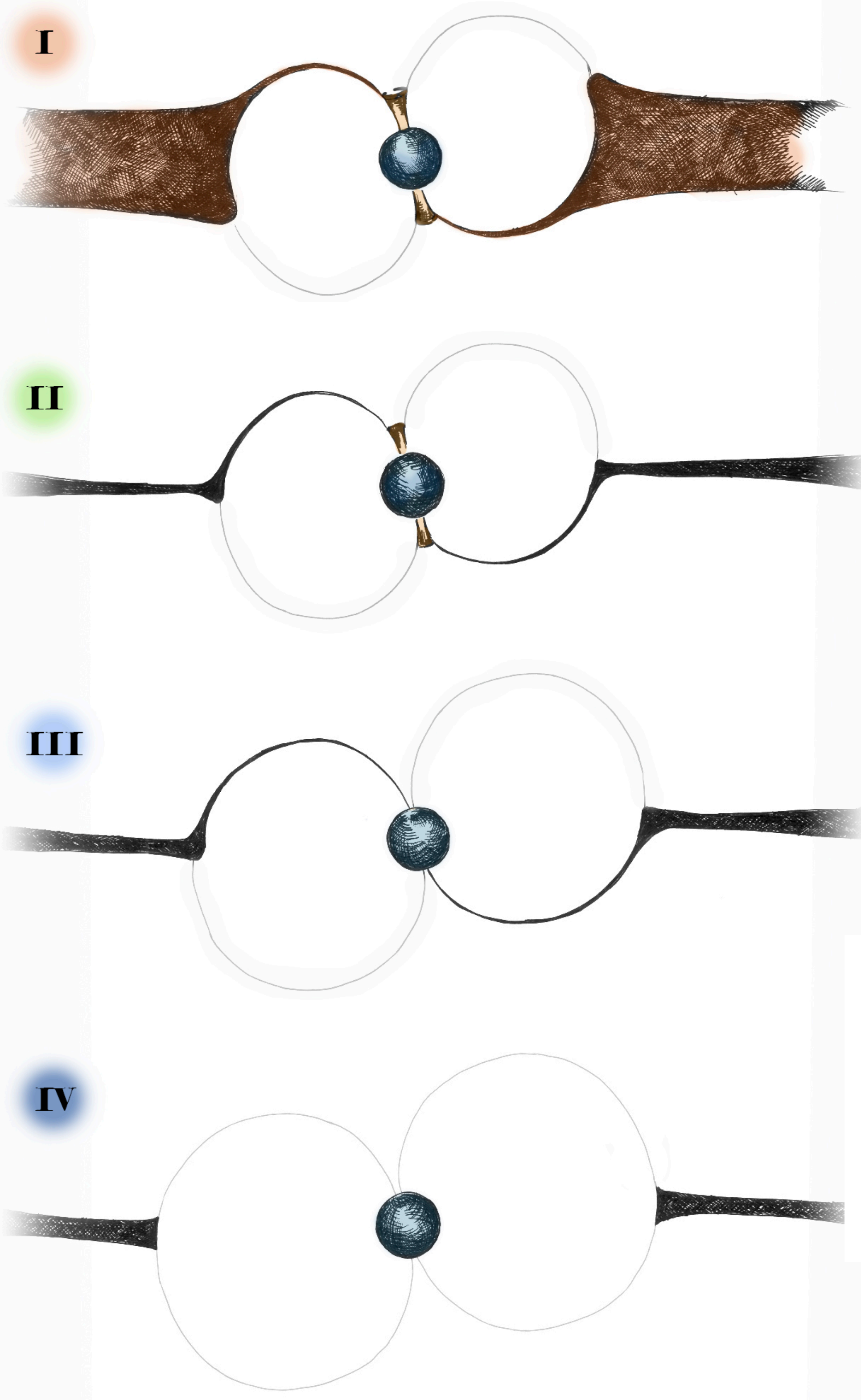

What happens at low luminosity state?

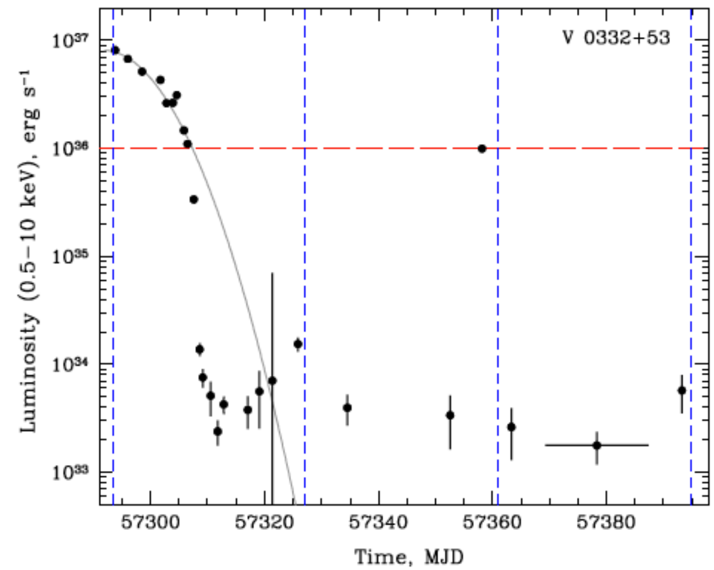

Illarionov&Sunyaev, 1975, A&A, 39
Tsygankov + 2016, A&A, 593

"propeller" effect
vs.
accretion from cold disc

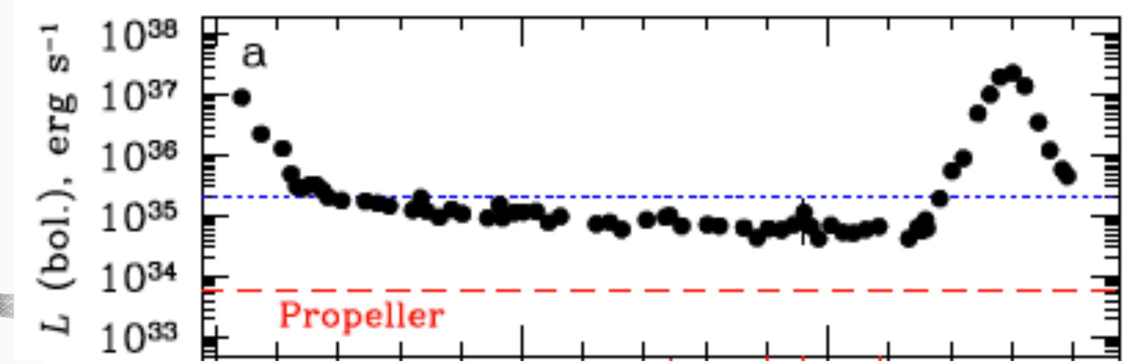

Tsygankov, AM+ 2017, A&A, 608

Observations:
Low luminosity state in GX 304-1

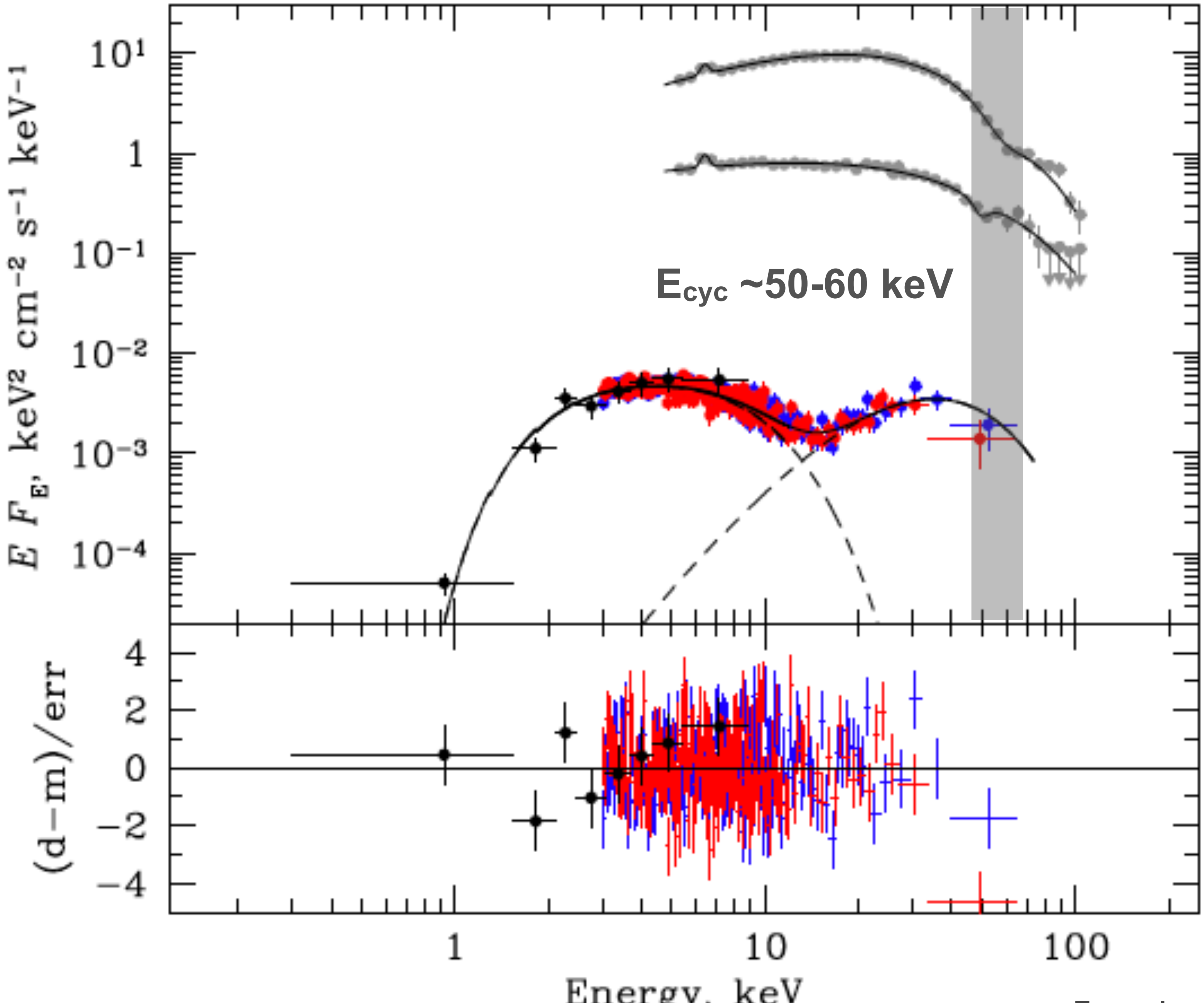

Tsygankov+, 2019, MNRAS,483L

Observations:
Low luminosity state in GX 304-1

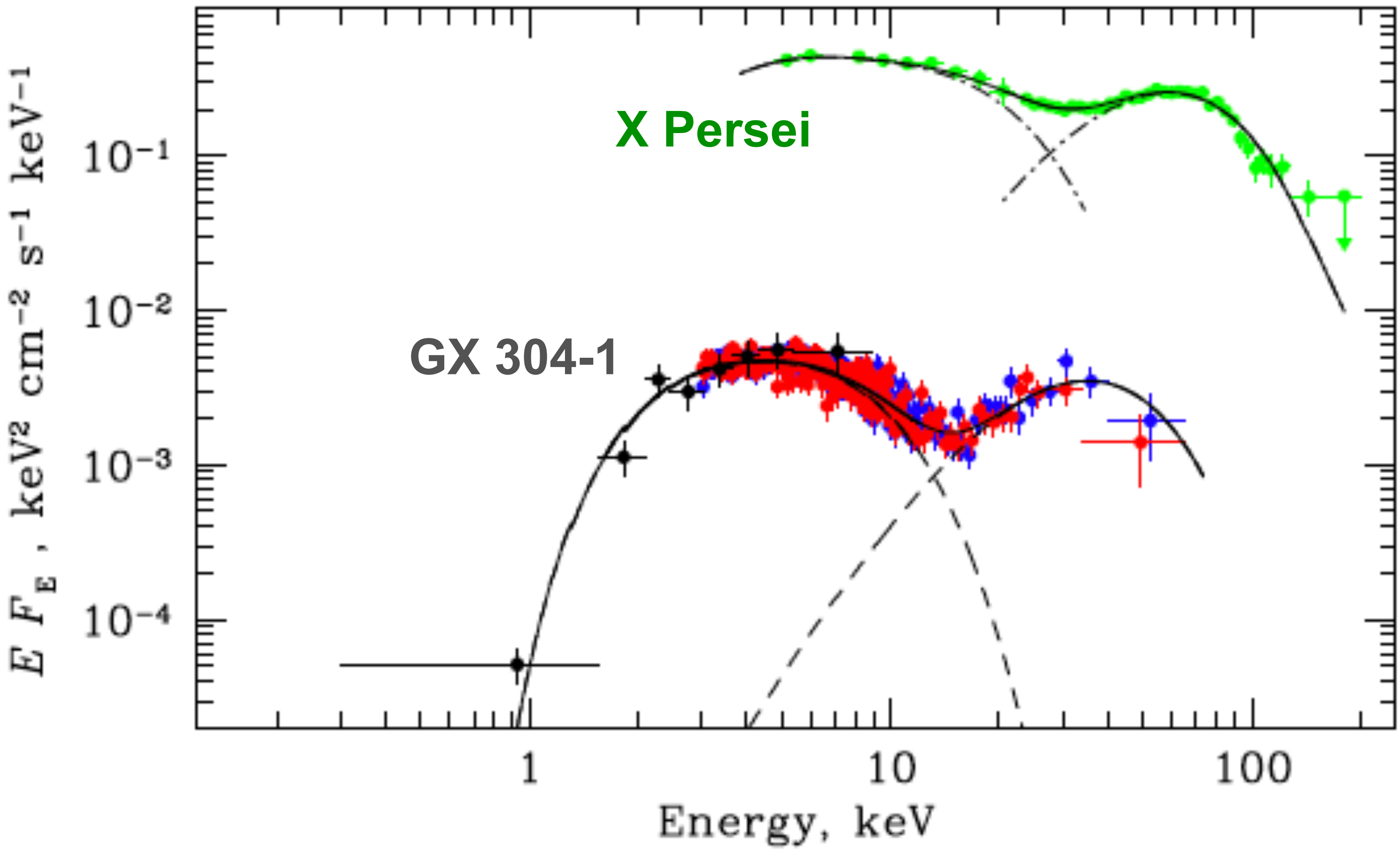

Doroshenko+, 2012, A&A,540

Tsygankov+, 2019, MNRAS,483L

Observations:
Low luminosity state in A 0535+262

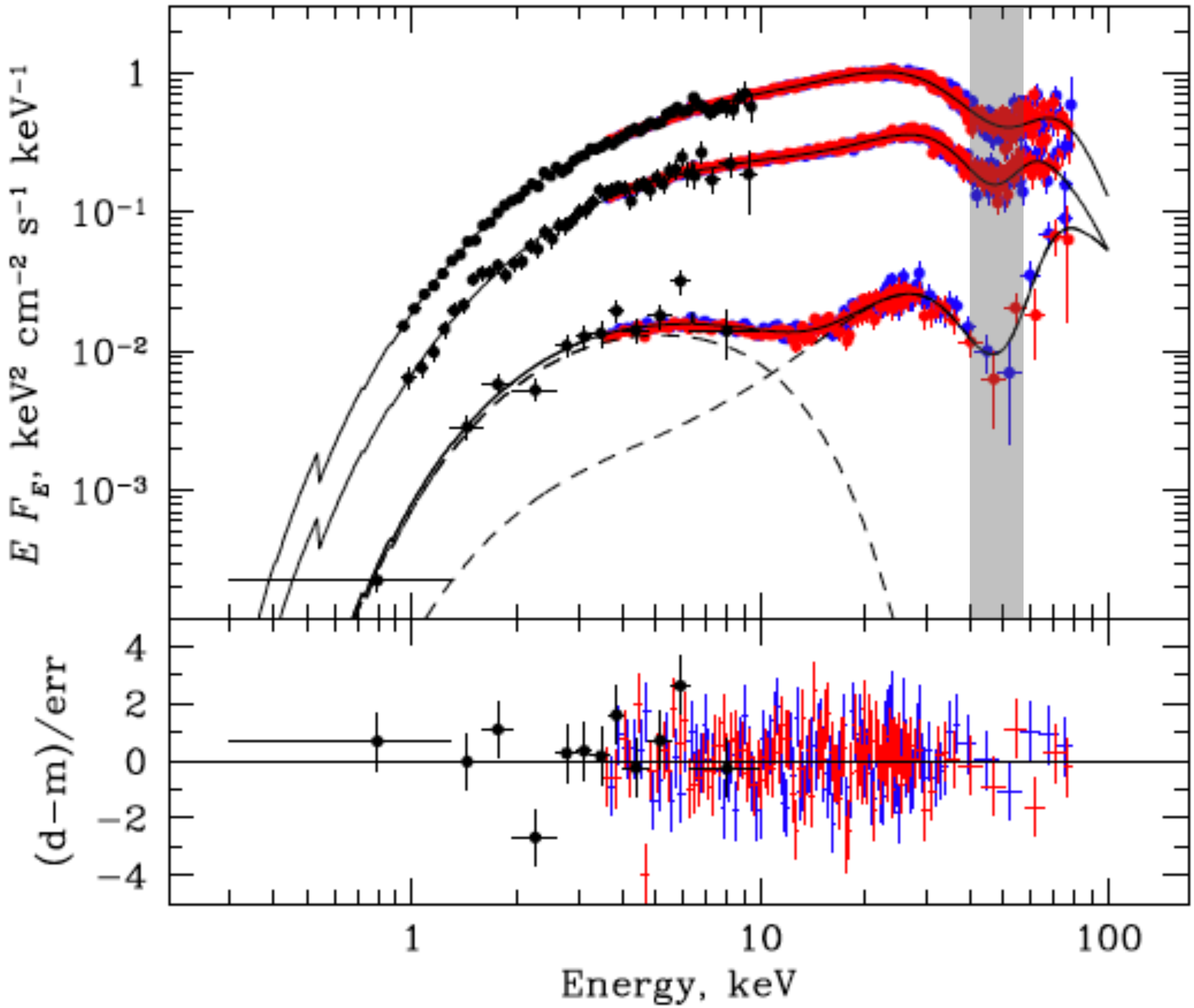

L ~ 2×10^{36} erg s^{-1}

L ~ 6×10^{35} erg s^{-1}

L ~ 7×10^{34} erg s^{-1}

Tsygankov+, 2019, MNRAS,487L

Observations:

Low luminosity state in X Persei, A0535+262 & GX 304-1

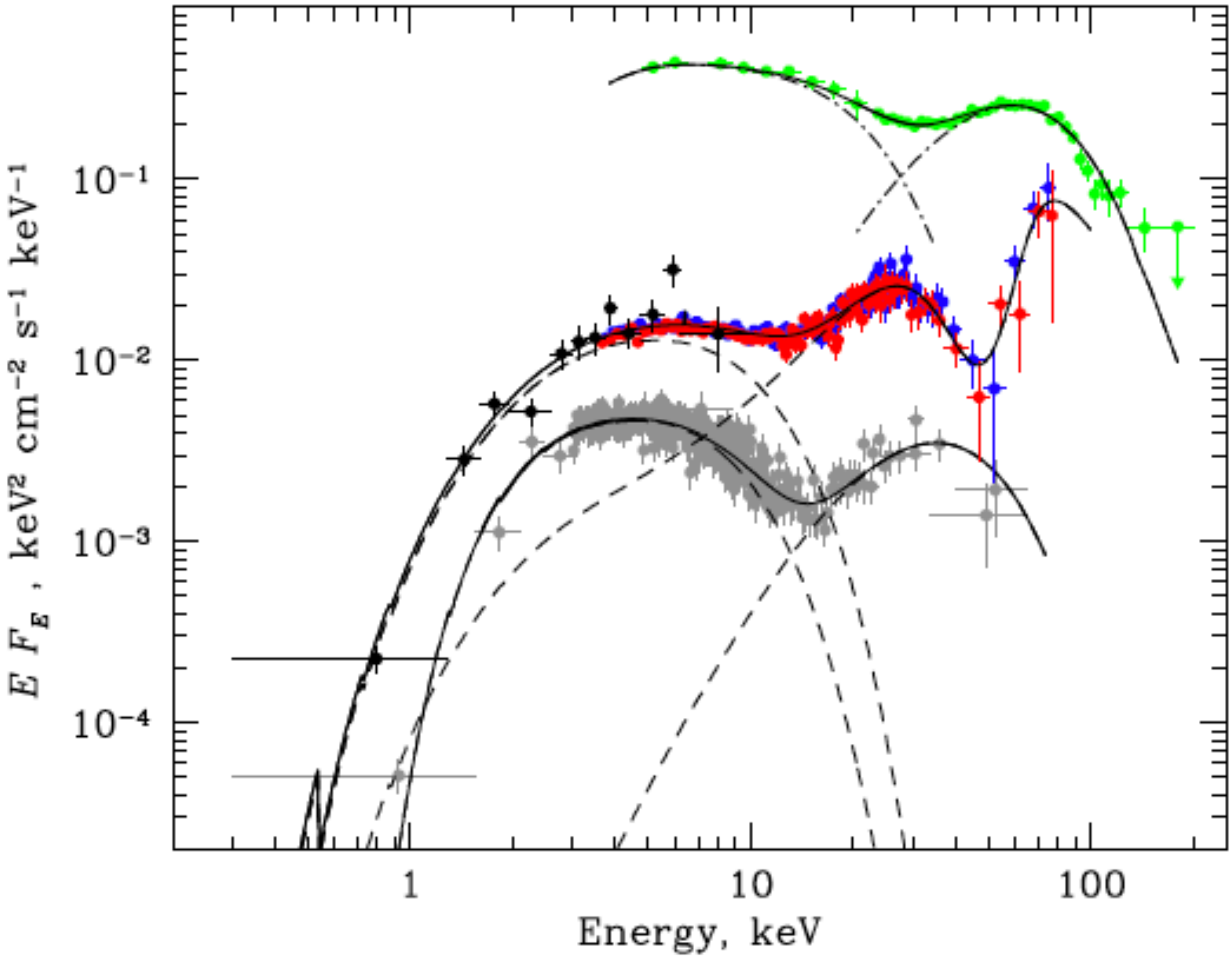

Tsygankov+, 2019, MNRAS,487L

What happens at low luminosity state?

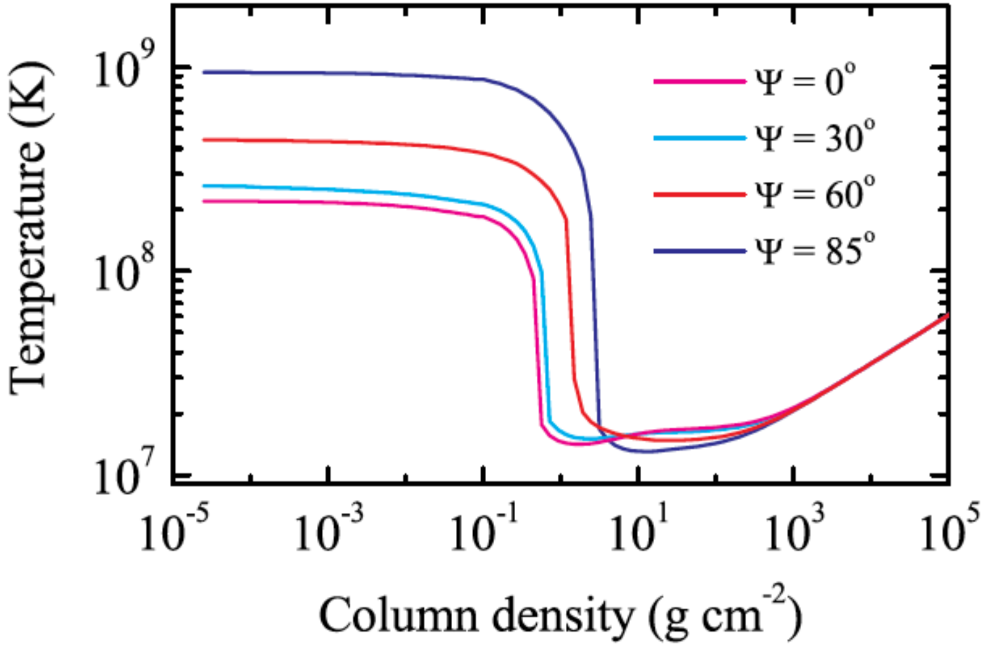

Suleimanov+, 2018, A&A

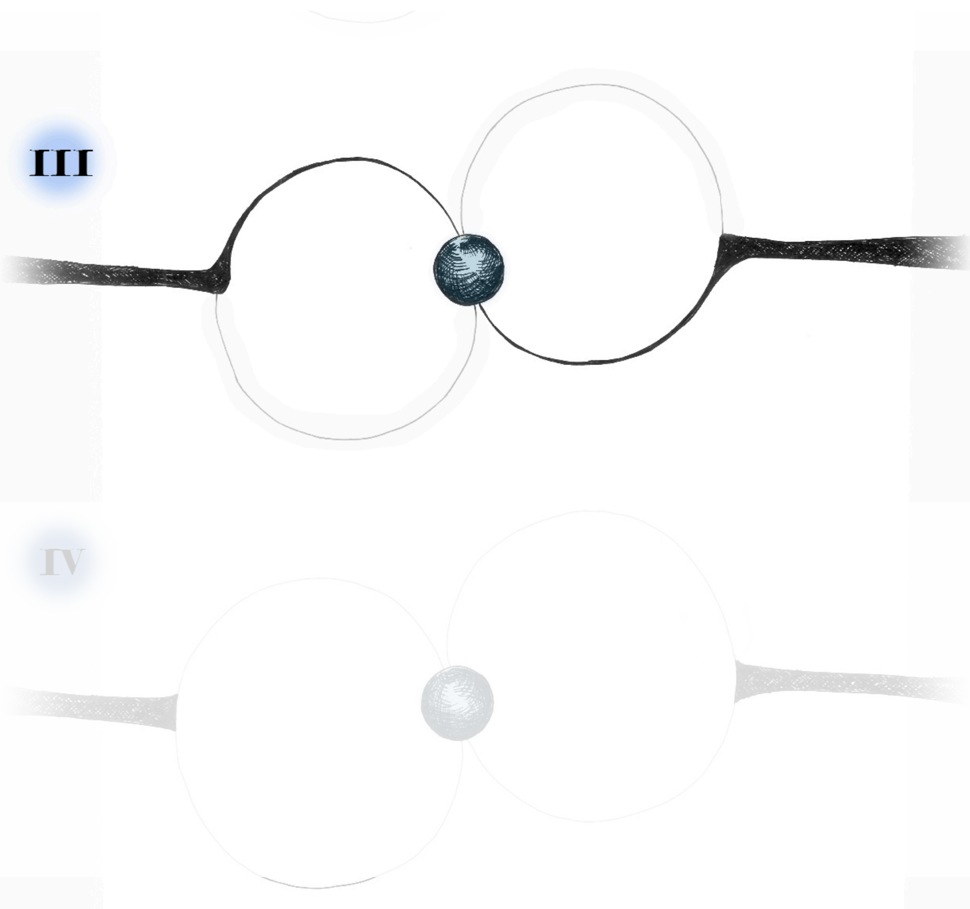

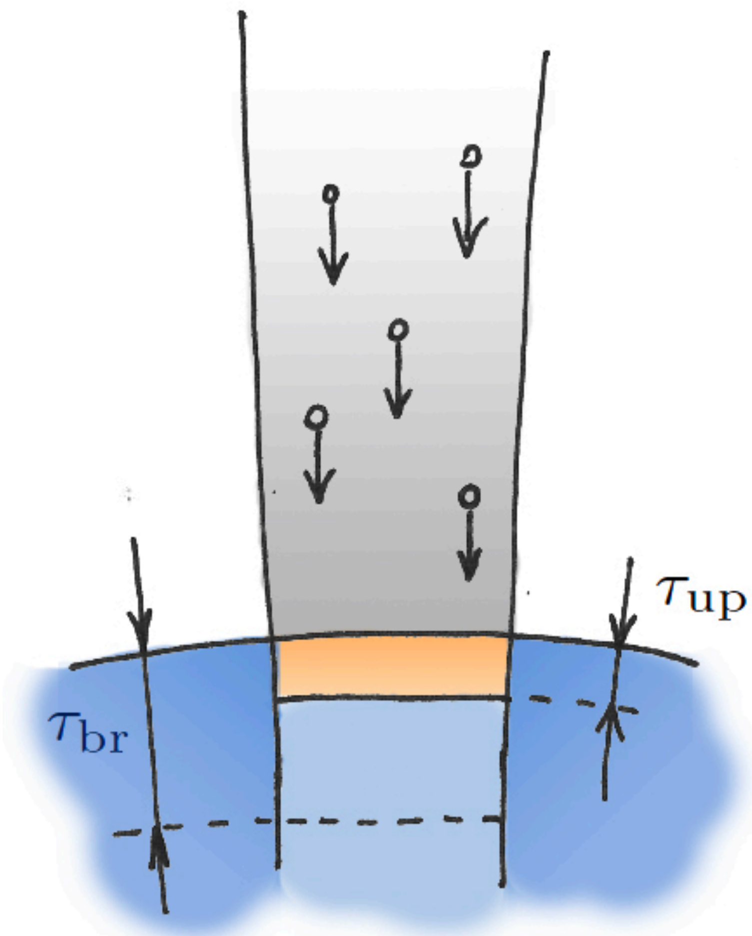

Physical model of spectra formation

$$\cos\theta \frac{\mathrm{d}I_E^{(j)}(\Omega)}{\mathrm{d}\tau_\mathrm{T}} = -\frac{\alpha_\mathrm{abs}^{(j)}(\Omega)}{\alpha_\mathrm{T}} I_E^{(j)}(\Omega) + \sum_{i=1}^{2} \int_0^\infty \mathrm{d}E' \int_{(4\pi)} \mathrm{d}\Omega' \left[R_{ji}(E,\Omega|E',\Omega') I_{E'}^{(i)}(\Omega') - R_{ij}(E',\Omega'|E,\Omega) I_E^{(j)}(\Omega) \right] + \frac{\alpha_\mathrm{abs}^{(j)}(E,\Omega)}{\alpha_\mathrm{T}} \frac{B_E}{2} + S_\mathrm{ini}^{(j)}(E,\Omega)$$

Absorption (bremsstrahlung and cyclotron absorption followed by electron collision)

+

Compton scattering

+

Cyclotron emission and Black Body

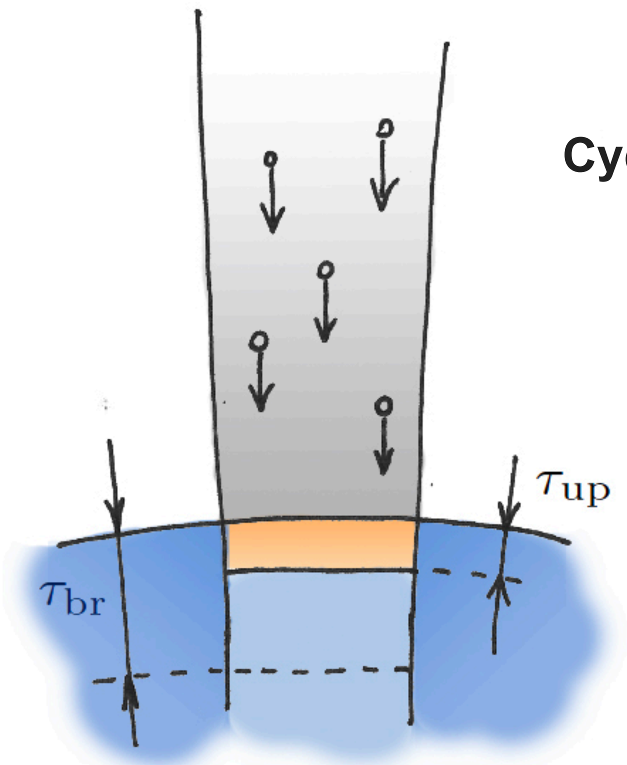

AM+,in prep.

Physical model of spectra formation

$$\cos\theta \frac{\mathrm{d}I_E^{(j)}(\Omega)}{\mathrm{d}\tau_\mathrm{T}} = -\frac{\alpha_\mathrm{abs}^{(j)}(\Omega)}{\alpha_\mathrm{T}} I_E^{(j)}(\Omega) + \sum_{i=1}^{2} \int_0^\infty \mathrm{d}E' \int_{(4\pi)} \mathrm{d}\Omega' \left[R_{ji}(E,\Omega|E',\Omega') I_{E'}^{(i)}(\Omega') - R_{ij}(E',\Omega'|E,\Omega) I_E^{(j)}(\Omega)\right] + \frac{\alpha_\mathrm{abs}^{(j)}(E,\Omega)}{\alpha_\mathrm{T}} \frac{B_E}{2} + S_\mathrm{ini}^{(j)}(E,\Omega)$$

Absorption (bremsstrahlung and cyclotron absorption followed by electron collision)

+

Compton scattering

+

Cyclotron emission and Black Body

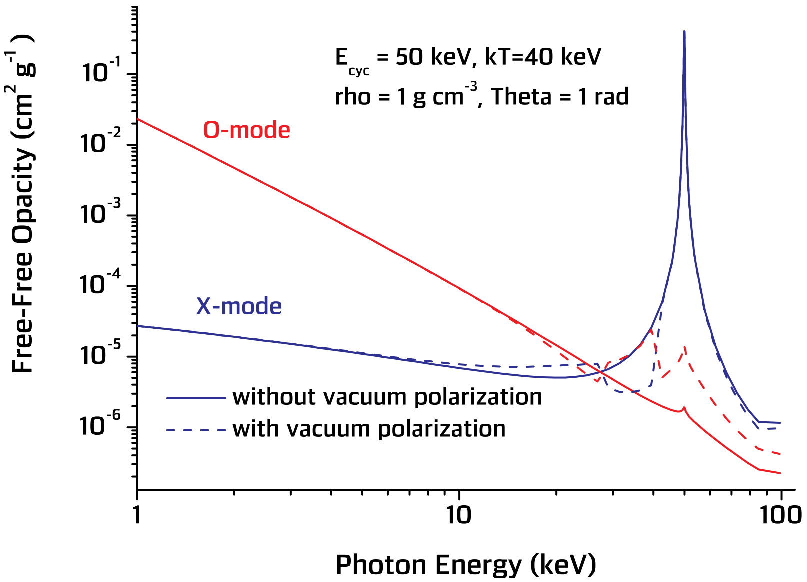

Probability of true cyclotron absorption:

$$P_\mathrm{abs,true} \simeq \frac{r_\mathrm{coll}}{r_\mathrm{cyc}} \sim 1.7\times10^{-7} n_{\mathrm{e},21} B_{12}^{-7/2}$$

AM+,in prep.

Physical model of spectra formation

$$\cos\theta \frac{\mathrm{d}I_E^{(j)}(\Omega)}{\mathrm{d}\tau_\mathrm{T}} = -\frac{\alpha_\mathrm{abs}^{(j)}(\Omega)}{\alpha_\mathrm{T}} I_E^{(j)}(\Omega)$$
$$+\sum_{i=1}^{2}\int_0^\infty \mathrm{d}E' \int_{(4\pi)} \mathrm{d}\Omega' \left[R_{ji}(E,\Omega|E',\Omega')I_{E'}^{(i)}(\Omega') - R_{ij}(E',\Omega'|E,\Omega)I_E^{(j)}(\Omega)\right]$$
$$+\frac{\alpha_\mathrm{abs}^{(j)}(E,\Omega)}{\alpha_\mathrm{T}}\frac{B_E}{2} + S_\mathrm{ini}^{(j)}(E,\Omega)$$

Absorption (bremsstrahlung and cyclotron absorption followed by electron collision)

+

Compton scattering

+

Cyclotron emission and Black Body

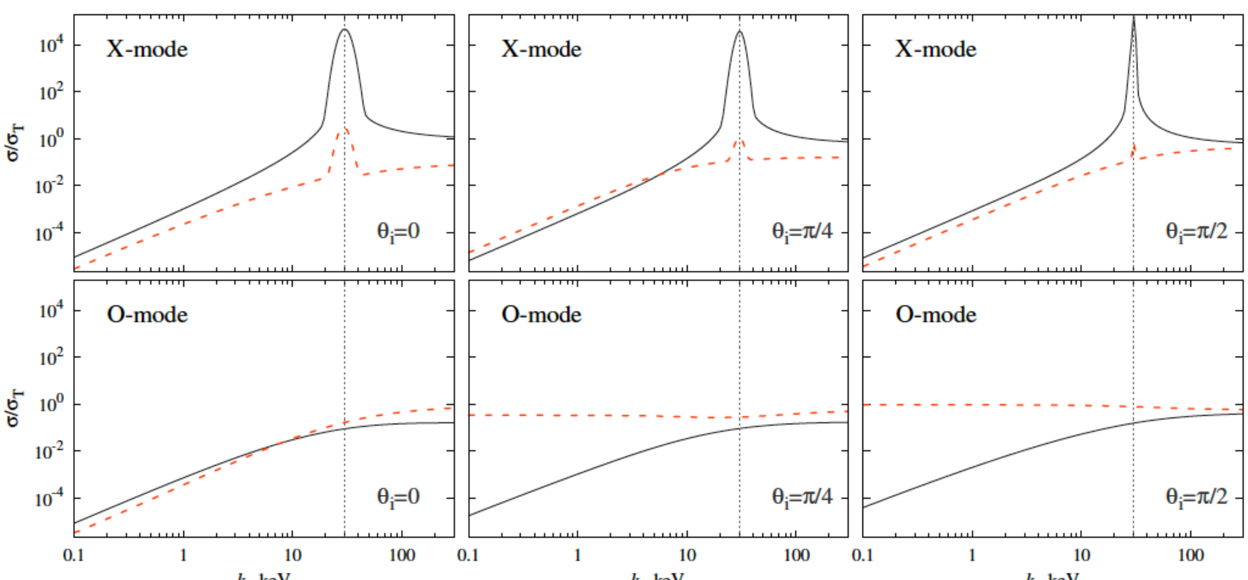

Cross-sections are based on non-relativistic amplitudes recalculated for plasma polarisation modes

AM+,in prep.

Physical model of spectra formation

$$\cos\theta \frac{\mathrm{d}I_E^{(j)}(\Omega)}{\mathrm{d}\tau_{\mathrm{T}}} = -\frac{\alpha_{\mathrm{abs}}^{(j)}(\Omega)}{\alpha_{\mathrm{T}}} I_E^{(j)}(\Omega)$$

$$+\sum_{i=1}^{2}\int_0^{\infty}\mathrm{d}E' \int_{(4\pi)} \mathrm{d}\Omega' \left[R_{ji}(E,\Omega|E',\Omega')I_{E'}^{(i)}(\Omega') - R_{ij}(E',\Omega'|E,\Omega)I_E^{(j)}(\Omega)\right]$$

$$+\frac{\alpha_{\mathrm{abs}}^{(j)}(E,\Omega)}{\alpha_{\mathrm{T}}}\frac{B_E}{2} + S_{\mathrm{ini}}^{(j)}(E,\Omega)$$

Absorption (bremsstrahlung and cyclotron absorption followed by electron collision)

+

Compton scattering

+

Cyclotron emission and Black Body

AM+,in prep.

Details of numerical simulations

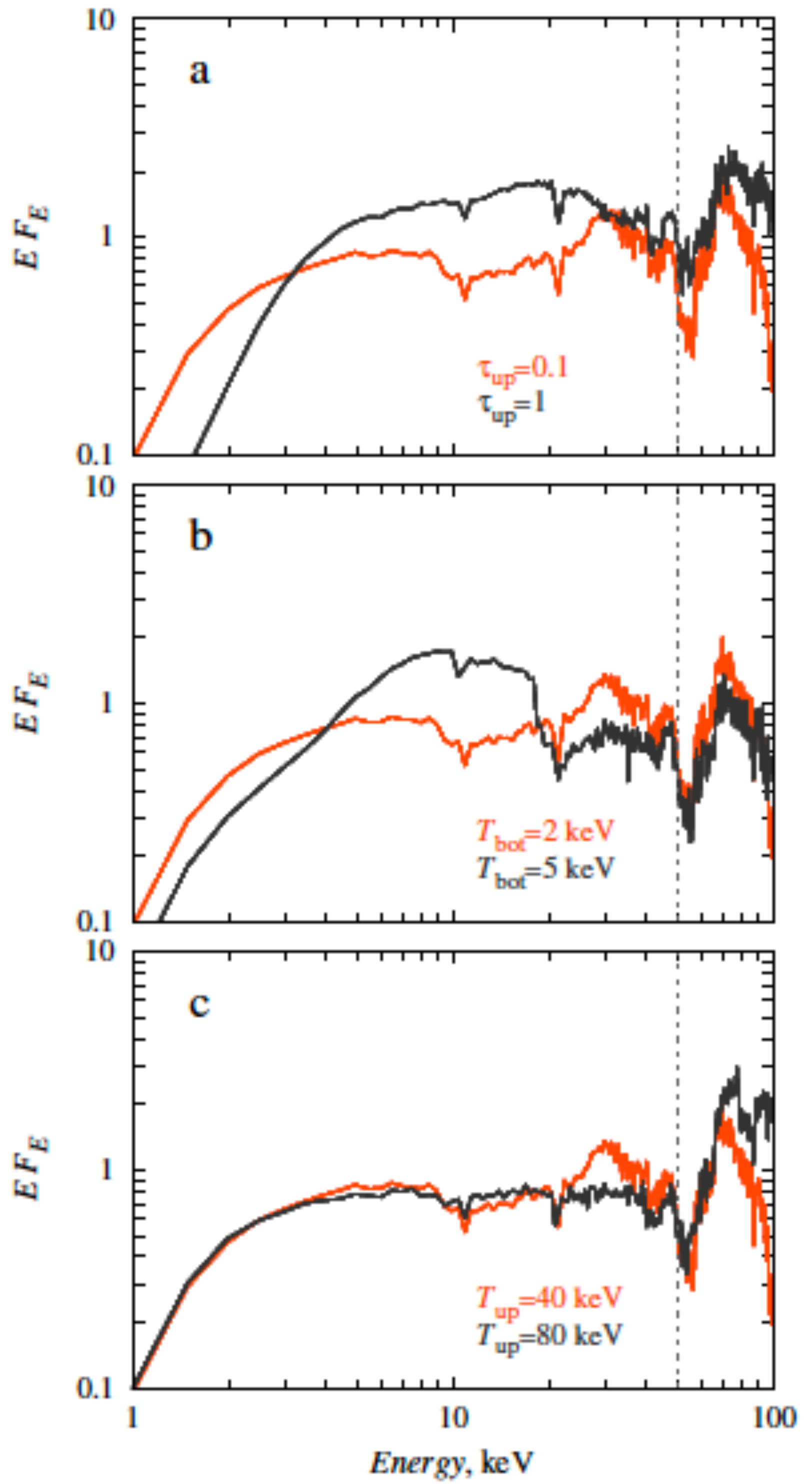

The basic parameters in the model:

(1) temperature of the upper layer **(T_{up})** and temperature below the upper layer **(T_{bot})**;

(2) optical thickness of the upper layer due to Thomson scattering **(τ_{up})**;

(3) effective depth where the accretion flow stopes in the atmosphere **(τ_{br})**.

$$E_{cyc} = 50\,\mathrm{keV}$$
$$T_{bot} = 2\,\mathrm{keV},\ T_{up} = 40\,\mathrm{keV}$$
$$\tau_{up} = 0.1,\ \tau_{br} = 1$$
$$Z = 1$$

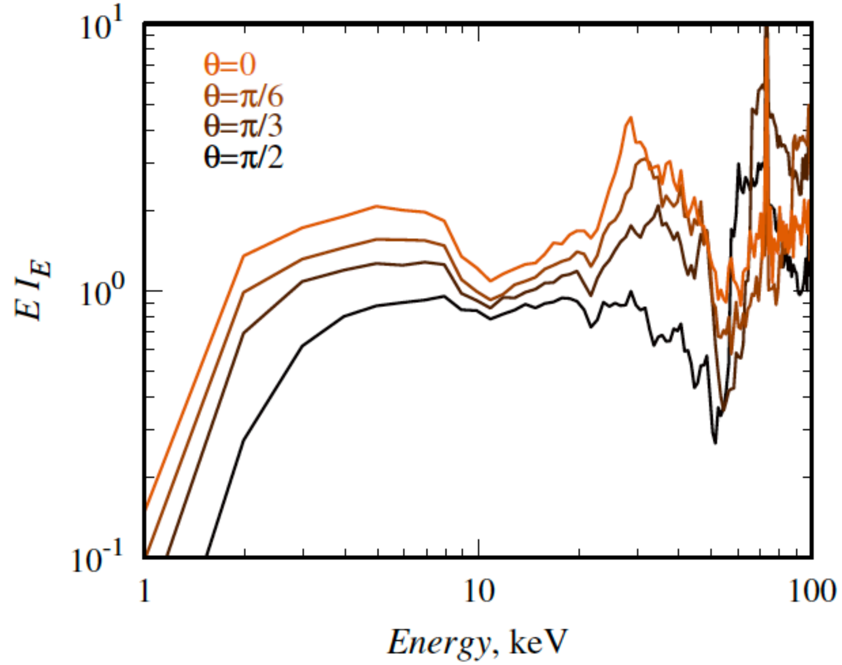

AM+,in prep.

Results of numerical simulations vs. Data

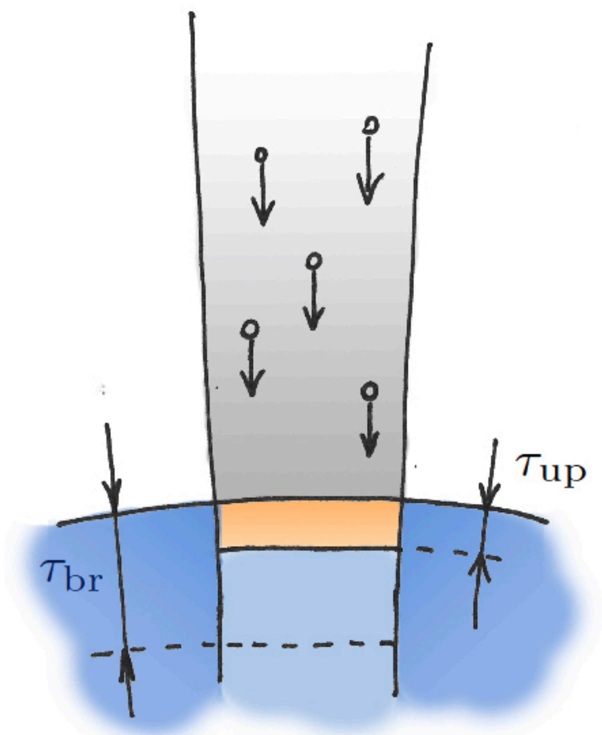

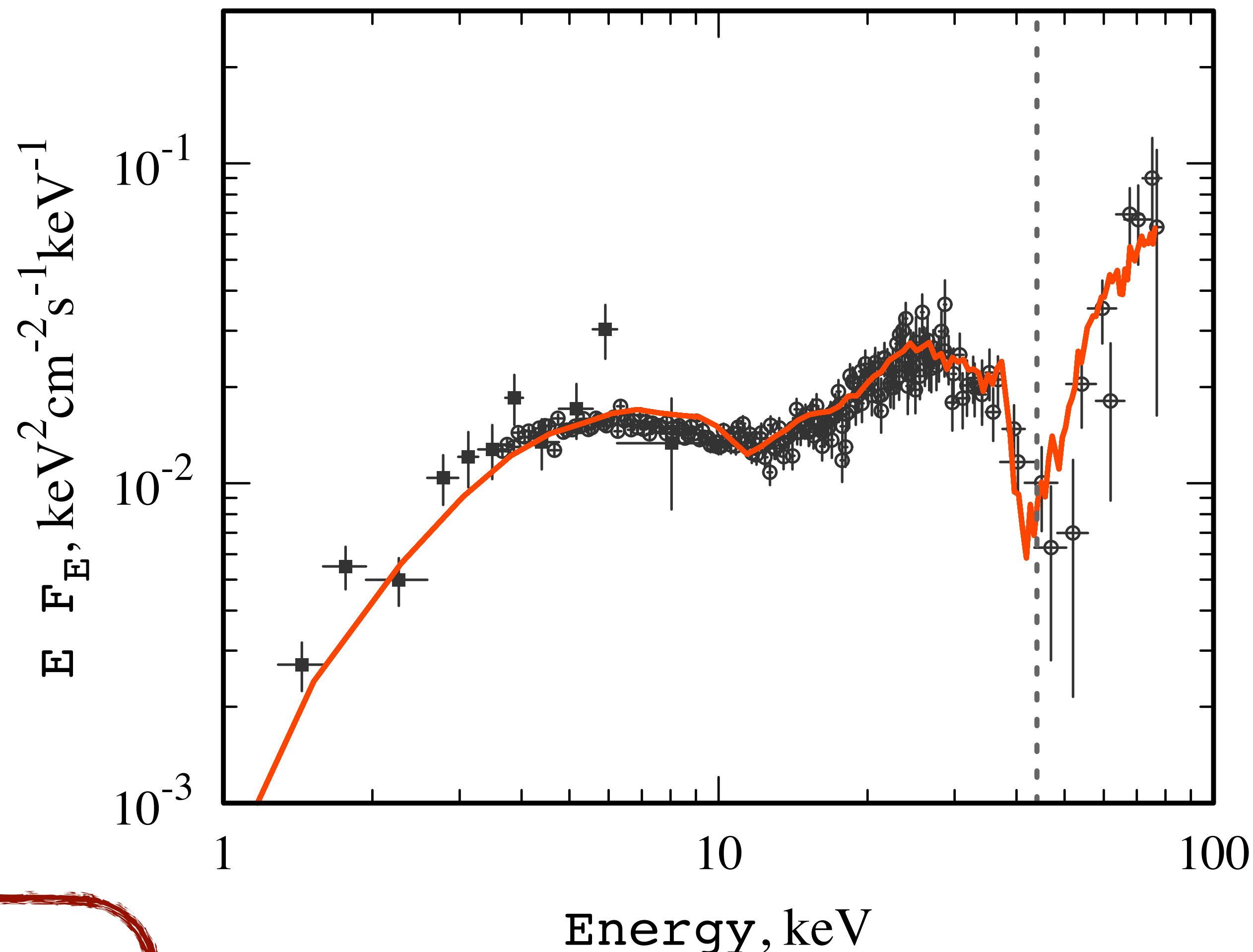

Set of Parameters:

$$\tau_{br} = 10$$

$$\tau_{up} = 0.5 \qquad T_{up} \approx 100\,keV$$

$$T_{down} \approx 2.7\,keV$$

AM+,in prep.

Conclusions

There is **dramatic changes** of X-ray energy spectra at very low luminosity states of X-ray pulsars. The spectra clearly **show two components**.

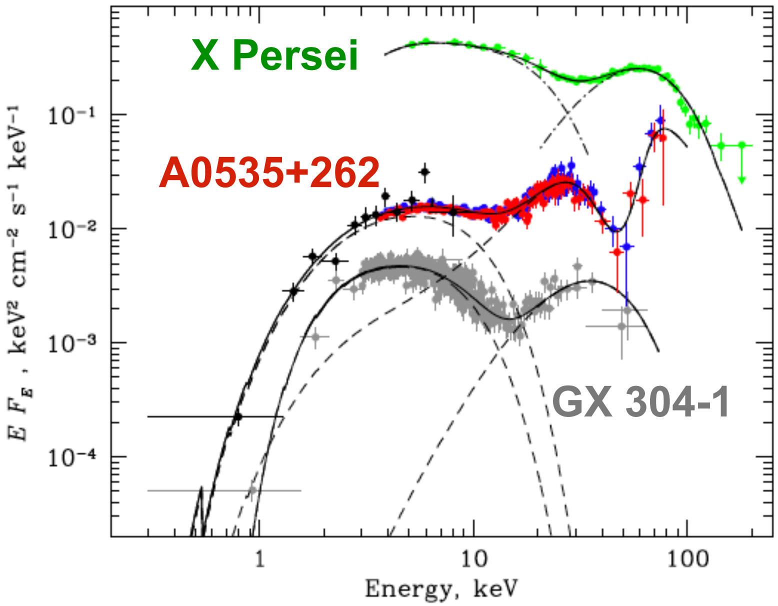

The observed spectra can be explained by cyclotron emission in the atmosphere of accreting neutron star with its further comptonisation affected by resonant scattering.

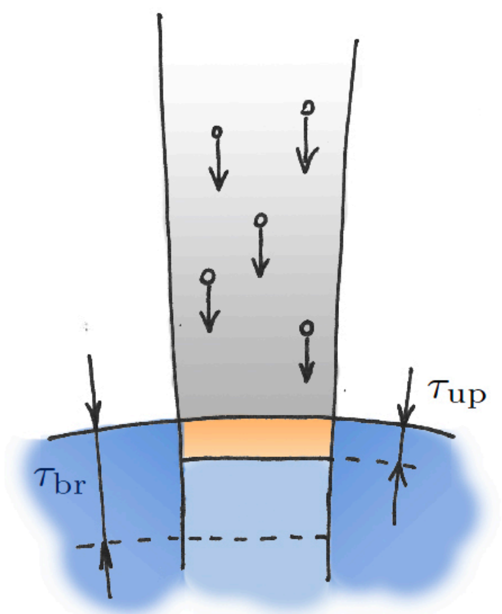

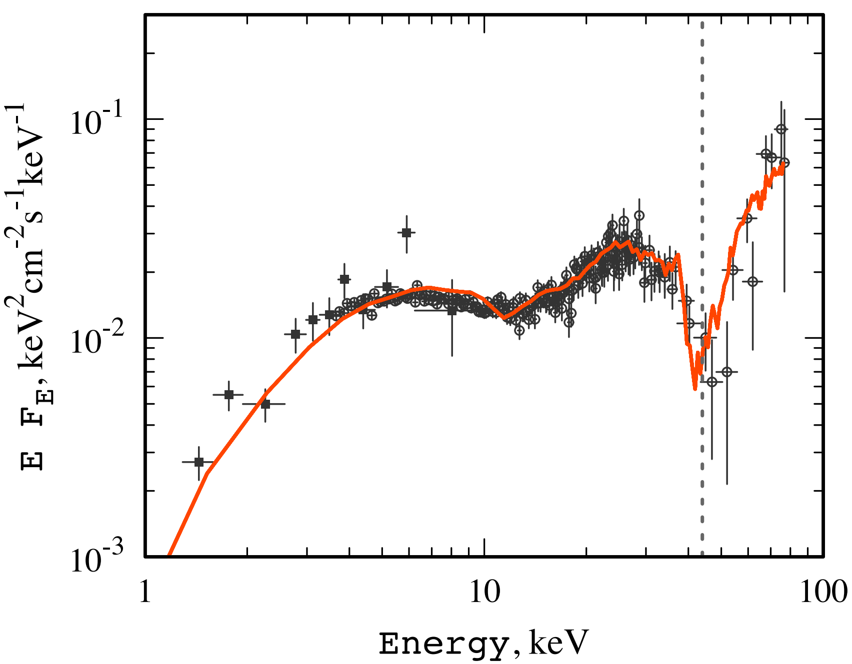

Spectra of X-ray pulsars at very low luminosity states can be used for estimations of magnetic field strength at the neutron star surface.

AM+,in prep.

Physical model of spectra formation

$$\cos\theta \frac{\mathrm{d}I_E^{(j)}(\Omega)}{\mathrm{d}\tau_\mathrm{T}} = -\frac{\alpha_\mathrm{abs}^{(j)}(\Omega)}{\alpha_\mathrm{T}} I_E^{(j)}(\Omega)$$
$$+\sum_{i=1}^{2}\int_0^\infty \mathrm{d}E' \int_{(4\pi)} \mathrm{d}\Omega' \left[R_{ji}(E,\Omega|E',\Omega') I_{E'}^{(i)}(\Omega') - R_{ij}(E',\Omega'|E,\Omega) I_E^{(j)}(\Omega)\right]$$
$$+\frac{\alpha_\mathrm{abs}^{(j)}(E,\Omega)}{\alpha_\mathrm{T}} \frac{B_E}{2} + S_\mathrm{ini}^{(j)}(E,\Omega)$$

Absorption (bremsstrahlung and cyclotron absorption followed by electron collision)

+

Compton scattering

+

Cyclotron emission and Black Body